

In Vivo Morphological Changes of the Femoropopliteal Arteries due to Knee Flexion After Endovascular Treatment of Popliteal Aneurysm

Journal of Endovascular Therapy
2019, Vol. 26(4) 496–504
© The Author(s) 2019
Article reuse guidelines:
sagepub.com/journals-permissions
DOI: 10.1177/1526602819855441
www.jevt.org
SAGE

Giovanni Spinella, MD, PhD¹ , Alice Finotello, PhD², Bianca Pane, MD¹, Giancarlo Salsano, MD³, Simone Mambrini, MD¹, Alexey Kamenskiy, PhD⁴, Valerio Gazzola, MD¹, Giuseppe Cittadini, MD³, Ferdinando Auricchio, PhD⁵, Domenico Palombo, MD¹, and Michele Conti, PhD⁵

Abstract

Purpose: To evaluate morphological changes of the femoropopliteal (FP) arteries due to limb flexion in patients undergoing endovascular treatment of popliteal artery aneurysms (PAAs). **Materials and Methods:** Seven male patients (mean age 68 years) underwent endovascular treatment of PAA with a Viabahn stent-graft between January 2013 and December 2017. During follow-up, one contrast-enhanced computed tomography angiography (CTA) scan of the lower limbs was acquired for each recruited patient. A standardized CTA protocol for acquisitions in both straight-leg and bent-leg positions was used to visualize changes in artery shape due to limb flexion. Three-dimensional reconstruction of the FP segment was performed to compute mean diameter and eccentricity of the vascular lumen and to measure length, tortuosity, and curvature of the vessel centerline in 3 arterial zones: (A) between the origin of the superficial femoral artery and the proximal end of the stent-graft, (B) within the stent-graft, and (C) from the distal end of the stent-graft to the origin of the anterior tibial artery. **Results:** After limb flexion, all zones of the FP segment foreshortened: 6% in zone A ($p=0.001$), 4% in zone B ($p=0.001$), and 8% in zone C ($p=0.07$), which was the shortest (mean 4.5 ± 3.6 cm compared with 23.8 ± 5.7 cm in zone A and 23.6 ± 7.4 cm in zone B). Tortuosity increased in zone A (mean 0.03 to 0.05, $p=0.03$), in zone B (0.06 to 0.15, $p=0.005$), and in zone C (0.027 to 0.031, $p=0.1$). Mean curvature increased 15% ($p=0.05$) in zone A, 27% ($p=0.005$) in zone B, and 95% ($p=0.06$) in zone C. In all zones, the mean artery diameter and eccentricity were not significantly affected by limb flexion. **Conclusion:** Limb flexion induces vessel foreshortening and increases mean curvature and tortuosity of the FP segment both within and outside the area of the stent-graft.

Keywords

endovascular treatment, femoropopliteal segment, foreshortening, limb flexion, medical image analysis, morphology, popliteal artery aneurysm, stent-graft, superficial femoral artery, tortuosity

Introduction

Popliteal artery aneurysms (PAAs) are the most frequently encountered peripheral aneurysms.¹ In elective cases, open or endovascular treatment is often used when the aneurysm reaches 2 cm in diameter.² Results of endovascular treatment were initially disappointing, likely due to the materials used in the first generation of devices,³ and while it continues to demonstrate lower patency rates compared with open repair using prosthetic materials or autologous vein,⁴ endovascular PAA repair is now indicated in selected cases.⁵ In particular, it is often used in the

¹Vascular and Endovascular Surgery Unit, Ospedale Policlinico San Martino, University of Genoa, Italy

²Department of Experimental Medicine, University of Genoa, Italy

³Department of Radiology, Ospedale Policlinico San Martino, Genoa, Italy

⁴Nebraska Medical Center, Omaha, NE, USA

⁵Department of Civil Engineering and Architecture, University of Pavia, Italy

Corresponding Author:

Giovanni Spinella, Vascular and Endovascular Surgery Unit, Ospedale Policlinico San Martino, University of Genoa, Largo Rosanna Benzi, 10–16132 Genoa, Italy.

Email: giovanni.spinella@unige.it

absence of arterial tortuosity and off-target area dilatation and when treating patients with at least 2 runoff vessels and proximal and distal stent-graft landing zones of at least 15 mm.⁶ However, clinical outcomes even in these selected patients are far from perfect, and treatment failures are often attributed to the severe repetitive deformations experienced by the femoropopliteal (FP) segment during limb flexion. These deformations can lead to kinking and compression of the endovascular device, contributing to thrombosis, stent fracture,⁷ and ultimately treatment failure.⁸ These considerations call for a quantification of the in vivo behavior of the FP arteries during limb flexion after endovascular aneurysm repair.

Until recently, only a few studies investigated FP kinematics in healthy patients^{9,10} or those with occlusive peripheral artery disease (PAD) *ex vivo*^{11,12} or in vivo using 2- or 3-dimensional (2D or 3D, respectively) angiography.^{13–15} Recently, Conti et al¹⁶ used 3D computed tomography angiography (CTA) to measure in vivo FP segment deformations during limb flexion and applied these data in a patient-specific stenting simulation. To the best of our knowledge, the in vivo assessment of post-stenting PAA deformations due to limb flexion has not yet been performed. Given this motivation, the present study aims at evaluating the morphological changes of the FP segment due to limb flexion in patients with endovascularly treated PAAs using a standardized protocol for CTA acquisition in both straight- and bent-limb positions.

Materials and Methods

Study Design

Patients with PAA who underwent stent-graft treatment were recruited in follow-up for an imaging study to identify the effects of limb flexion on popliteal artery deformation. Signed informed consent was obtained from all patients and all procedures were performed in accordance with the Declaration of Helsinki and submitted to the local institutional medical ethics committee. Patients were eligible for endovascular PAA treatment if the proximal and distal landing zones were at least 15 mm long, the artery was relatively straight and free from stenosis or off-target dilatation, and there was at least 2-vessel runoff. For this study, patients could be of either sex and between 50 and 85 years old, but without contraindications to CTA. Other exclusion criteria were previous peripheral surgical or endovascular procedures, inability to give signed informed consent, and PAA stent-graft occlusion during follow-up.

Endovascular Treatment

Endovascular PAA treatment with the Viabahn self-expanding stent-graft (W.L. Gore & Associates, Flagstaff,

AZ, USA) was planned on the basis of preoperative CTA. The stent-graft was oversized 10% with respect to the proximal landing zone diameter; no oversizing was used for the distal landing zone. Because of tapering of the artery distally, 2 or 3 stent-grafts were placed to avoid excessive oversizing, and the length of these stent-grafts was chosen in accordance with the length necessary to exclude the aneurysm.

All patients were treated under spinal anesthesia. Surgical exposure of the proximal superficial femoral artery (SFA) was performed, and a 10-F to 11-F introducer was placed after systemic heparinization. Angiographic images were acquired, and a stiff guidewire (Supra Core; Abbott Vascular, Redwood City, CA, USA) was placed in the tibial or below-knee arteries. The endografts were then deployed, and angiography was repeated to ensure correct placement. Patients were discharged on dual antiplatelet therapy (clopidogrel 75 mg/d and aspirin 100 mg/d), which should be prescribed lifelong.

Imaging Acquisition Protocol

During follow-up, one contrast-enhanced CTA of the lower limbs was acquired in each recruited patient in addition to the routine color Doppler imaging. During this CTA examination, 2 scans were performed a few minutes apart. During the first scan, the treated lower limb was placed in the standardized 90° position (bent-leg configuration) using a dedicated foam-coated leg support (Figure 1A), while the contralateral limb remained straight. Following bent-limb imaging, the treated limb was placed in the 180° position (straight-leg configuration) to acquire the second scan (Figure 1B). All CTA images were acquired with the same 64 multidetector-row CTA scanner (Optima 660; General Electric Medical Systems, Milwaukee, WI, USA). The adopted scan parameters were: 0.625-mm thickness, 0.625-mm increment, 64×0.625 collimation, 0.915 pitch, 0.7-second rotation time, 35-cm field of view, and a 512×512-pixel matrix. A low-dose radiation protocol was used, with 100 keV and automated tube current modulation.

In each patient, an 18-G intravenous catheter was placed in an antecubital vein in the upper limb, and contrast material was injected using a double-syringe injector. Contrast [50–70 mL of iomeprol 400 or iopamidol 370 (BYK, Paris, France)] was administered at a flow rate of 4 mL/s followed by a 30-mL saline flush at 4 mL/s. The start trigger of scanning was individually obtained for each patient by using the “smart prep” technique, with a trigger level of 100 Hounsfield units and a delay time of 5 seconds to obtain optimal intraluminal contrast enhancement. The triggering area was manually placed at the aortic hiatus. The first scan was obtained in a single breath-hold from the aortic hiatus to dorsalis pedis artery (DPA) with the treated lower limb at the 90° position. The second scan was obtained from the

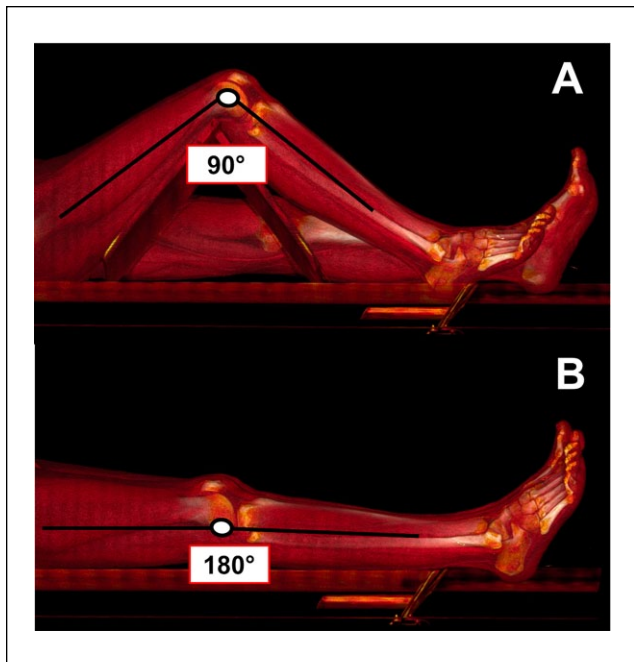


Figure 1. Computed tomography angiography acquisition in standardized (A) bent-leg and (B) straight-leg positions.

common femoral artery to DPA with the treated lower limb at 180° position.

Image Processing

Postoperative CTA images were anonymized and transferred to a workstation for image processing. Segmentation of the vessels from the femoral artery bifurcation to the popliteal artery bifurcation, leg bones, calcifications of the arterial wall (if present), and the implanted stent-graft was performed using the open source Vascular Modeling ToolKit (VMTK),¹⁷ a library of methods specifically conceived for the image segmentation and processing of vascular structures. This tool allows creation of an automated framework, consisting of a pipeline of instructions that minimizes users' interaction by limiting it to the segmentation phase alone. The adopted segmentation algorithm was previously validated using a patient-specific carotid phantom.¹⁷ For each patient, rigid registration of bent-leg structures on their corresponding straight counterparts was automatically performed by means of the Iterative Closest Point algorithm¹⁸ implemented in VMTK.

Reconstruction of the vessel centerline was performed automatically¹⁹ followed by resampling and smoothing operations using the moving average filter. The FP segment was then divided into 3 zones (Figure 2) spanning the distance between the SFA origin and the proximal end of the

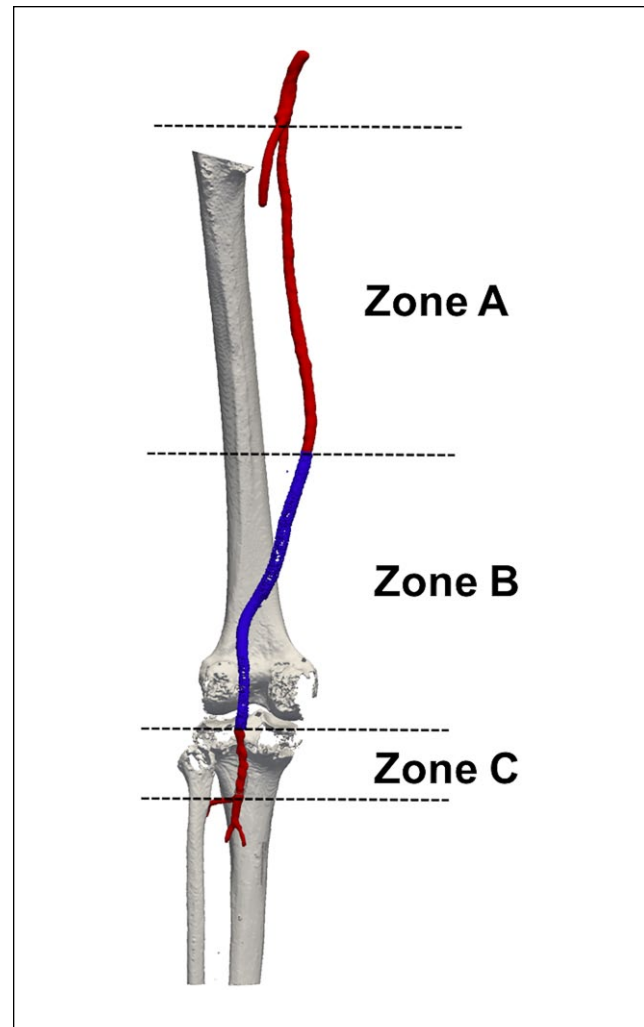


Figure 2. Subdivision of the femoropopliteal segment into 3 zones: (A) between the origin of the superficial femoral artery (red) and the proximal end of the stent-graft (blue), (B) from the proximal to the distal end of the stent-graft (blue), and (C) from the distal end of the stent-graft to the origin of the anterior tibial artery (red).

stent-graft (zone A), from the proximal to the distal end of the stent-graft (zone B), and from the distal end of the stent-graft to the origin of the anterior tibial artery (zone C). Since all stent-grafts were placed in the popliteal artery, in many subjects, zone C was the shortest of all 3 zones.

For each zone, the following parameters were automatically computed by means of VMTK scripts: centerline length, centerline pointwise curvature, centerline global tortuosity, diameter, and eccentricity of each section along the vessel centerline. Each of the computed parameters was compared between straight- and bent-leg configurations.

A foreshortening index (FI) was defined based on centerline length as

$$FI[\%] = \frac{\text{length}_{\text{bent}} - \text{length}_{\text{straight}}}{\text{length}_{\text{straight}}} \times 100$$

to quantify the difference in length between the 2 limb flexion configurations. When 2 or more stent-grafts overlapped, the length of the overlapping zone was measured as well. Starting from the vessel centerline, equally spaced planes perpendicular to the centerline were computed, and diameter and eccentricity measurements were taken on each transverse section. Maximum cross-sectional diameter was measured to detect zones of partial stenosis/thrombosis. Then, for each of the 3 zones (A, B, and C), mean and minimum values were extracted. Section eccentricity was calculated to assess flexion-induced cross-sectional pinching defined for each cross-section as: $E=d/D$, where d and D are the minimum and maximum diameters of the artery, respectively. Absolute mean and minimum values for each zone (A, B, and C) were then extracted.

The tortuosity index was measured as a global parameter, describing the overall shape of the vessel. Curvature was computed for each point of the centerline representing the local behavior of the centerline. For both straight- and bent-limb configurations, the tortuosity index was defined as: $T=L/ED - 1$, where L represents the centerline length and ED is the shortest distance between the 2 centerline endpoints. This parameter quantifies the fractional increase in length of a tortuous vessel compared with a perfectly straight path. Curvature of the vessel centerline was defined for each point of the centerline as the inverse of the radius of the osculating circle, ie, the circle that approximates the curve at a given point. An automatic script implemented in VMTK was adopted to compute pointwise curvature values along the centerline,²⁰ and the maximum value of curvature was then calculated.

Patient Sample

During the 5-year study period, 29 patients with PAA underwent stent-graft repair at a single center. Of these, 7 male patients (mean age 68 years) gave informed consent to participate in the study. Patient demographics and comorbidities are listed in Table 1. The proximal landing zone of the stent-graft was either in the SFA or proximal popliteal artery, while the distal landing zone was in the popliteal artery below the knee at an average 45.2 ± 35.6 mm distance from the origin of the anterior tibial artery. Mean CTA follow-up was 17.8 months (range 1–57) at the time of the follow-up CTA; all scans were successfully segmented both in the straight- and the bent-limb configurations (Figure 3). Since the arteries were not heavily calcified, analysis of calcification was not performed.

Table 1. Characteristics of the 7 Study Patients.^a

Age, y	67.8±9.5
Men	7
Smoking	3
Hypertension	7
Diabetes	3
COPD	4
Ischemic cardiomyopathy	5
Chronic renal failure	2
ASA 1, 2	2
ASA 3, 4	5

Abbreviations: ASA, American Society of Anesthesiologists; COPD, chronic obstructive pulmonary disease.

^aContinuous data are presented as the mean ± standard deviation; categorical data are given as the number.

Statistical Analysis

Two independent skilled observers performed segmentation of CTA images, followed by centerline computation and extraction of diameter and curvature measurements. One observer performed segmentation twice allowing for interobserver and intraobserver variability analyses using the intraclass correlation coefficient (ICC). Results are presented with the 95% confidence interval (CI).

Categorical variables are expressed as absolute frequencies, whereas continuous variables are given as means ± standard deviations. Differences between the bent- and straight-limb configurations were analyzed using a paired-sample t test; $p < 0.05$ was considered statistically significant. All statistical analyses were performed using the JMP software (version 13.0; SAS Institute, Cary, NC, USA).

Results

Arterial diameters, eccentricity, length, tortuosity, and curvature for each of the 3 FP zones in straight- and bent-limb configurations are reported in Table 2. Zone A on average foreshortened 6% from 238.5 ± 56.77 to 225.21 ± 56.87 mm during limb flexion ($p=0.001$); the curvature and tortuosity increased 15% ($p=0.05$) and 67% ($p=0.03$), respectively. No significant changes in minimum or mean diameters or eccentricity between the straight- and bent-limb configurations were observed.

Stent-grafted zone B on average foreshortened 4%, from 236.36 to 226.08 mm with limb flexion ($p=0.001$); when devices overlapped, the length of the overlap decreased 9% due to limb flexion. Similar to zone A, limb flexion produced a significant increase (27%, $p=0.005$) in mean curvature (from 0.026 to 0.033 on average) and a significant increase (150%, $p=0.005$) in tortuosity (0.06 to 0.15 on average). The difference in mean and minimum diameters

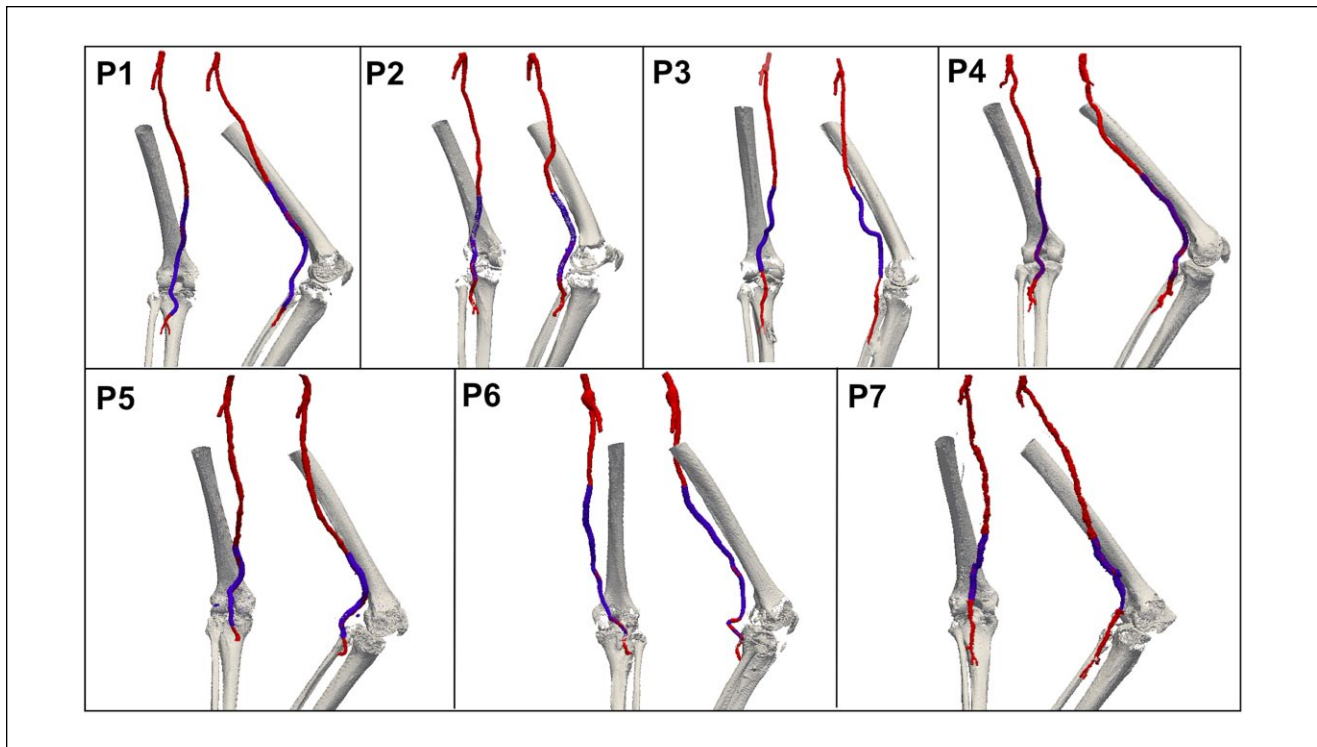


Figure 3. Three-dimensional reconstructions of the femoropopliteal segment (red), stent-graft (blue), and bones (gray) in 7 patients (P) recruited for this study. Two different views are presented for each patient.

Table 2. Measurements in Straight-Leg and Bent-Leg Positions in Zones A, B (Repaired), and C.

	Straight-Leg	Bent-Leg
Zone A		
Mean diameter, mm	8.25±1.10	8.15±0.90
Minimum diameter, mm	7.41±1.35	7.30±0.98
Eccentricity	0.89±0.01	0.90±0.01
Minimum eccentricity	0.75±0.06	0.73±0.05
Length, mm	238.50±56.77	225.21±56.87
Tortuosity	0.03±0.01	0.05±0.02
Mean curvature, 1/mm	0.027±0.007	0.031±0.005
Zone B		
Mean diameter, mm	7.42±1.08	7.12±0.94
Minimum diameter, mm	6.08±1.81	5.89±1.70
Eccentricity	0.9±0.02	0.89±0.02
Minimum eccentricity	0.75±0.08	0.70±0.08
Length, mm	235.36±74.24	226.08±72.77
Tortuosity	0.06±0.03	0.15±0.09
Mean curvature, 1/mm	0.026±0.005	0.033±0.006
Zone C		
Mean diameter, mm	6.65±0.87	6.60±1.01
Minimum diameter, mm	6.64±1.66	6.50±1.78
Eccentricity	0.88±0.04	0.89±0.05
Minimum eccentricity	0.76±0.07	0.70±0.13
Length, mm	45.20±35.61	42.35±30.99
Tortuosity	0.027±0.017	0.031±0.01
Mean curvature, 1/mm	0.032±0.013	0.063±0.034

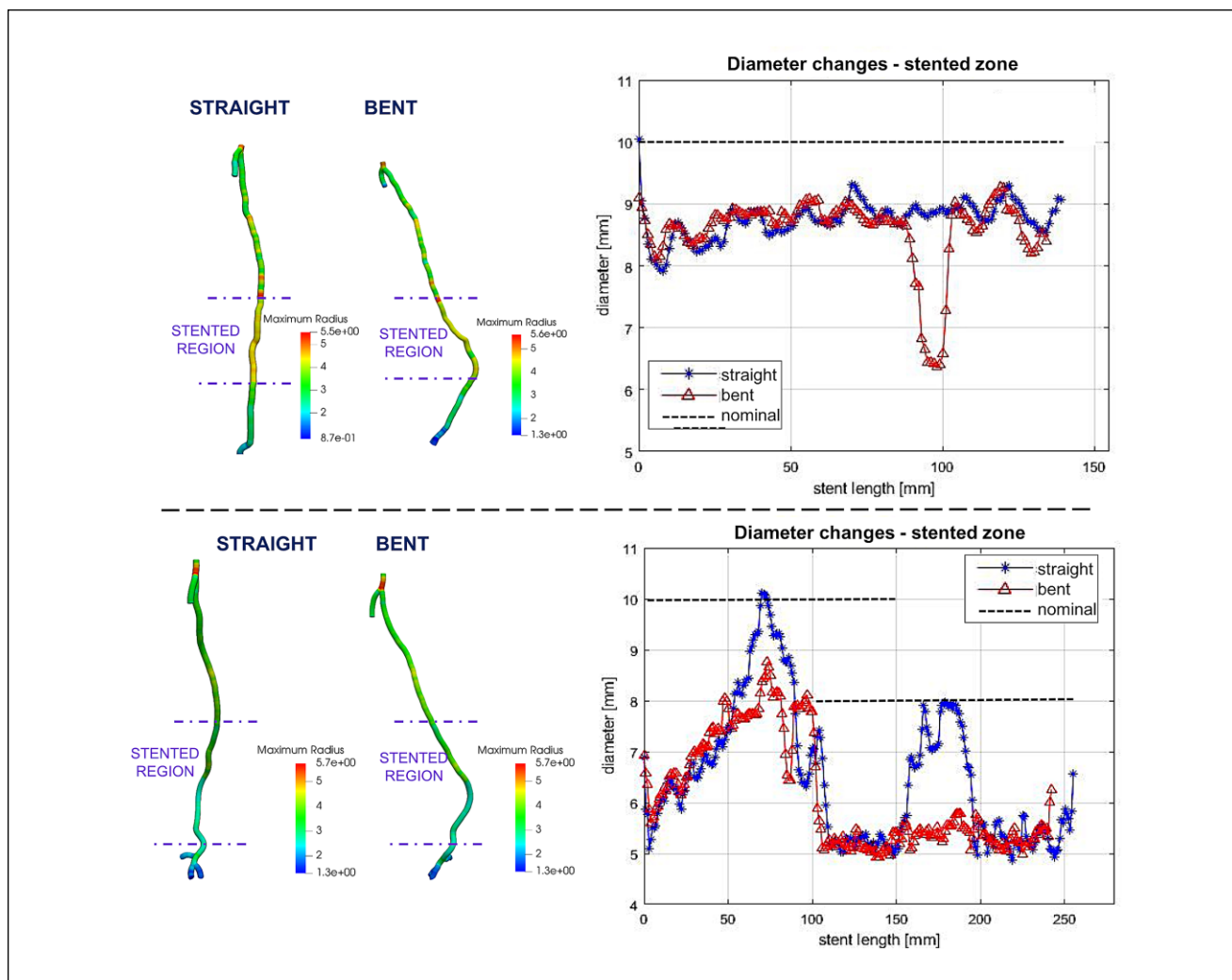


Figure 4. Diameter reduction in the stent-graft segment due to limb flexion in 2 patients. Left: Contour plots depicting changes in artery diameter along the length of the segmented femoropopliteal arteries. Right: Change in femoropopliteal diameter along the length of the stent-graft zone in straight (blue) and bent (red) positions. Nominal stent-graft diameters are depicted with black dashed lines; 2 partially overlapping endografts are shown for the second patient.

between the straight-leg and bent-leg positions was not statistically significant, but localized areas of diameter reduction in the stent-grafted zone in the bent-leg position were observed in 2 patients (Figure 4). Average eccentricity was not affected by leg flexion, and minimum eccentricity decreased from 0.74 ± 0.08 to 0.70 ± 0.08 but statistical significance was not reached ($p=0.9$). The most severe changes in minimum eccentricity were observed in 2 patients (from 0.72 to 0.59 and from 0.84 to 0.6, respectively; Figure 5).

Zone C was 5-fold shorter (mean 4.5 ± 3.6 cm with extended leg) than zones A (23.8 ± 5.7 cm) or B (23.6 ± 7.4 cm). Zone C foreshortened the most (8%) during limb flexion, but this result did not reach statistical significance ($p=0.07$), nor were there significant differences in length, diameter, tortuosity, or eccentricity with limb flexion.

Intraobserver and Interobserver Reproducibility

Intraobserver ICC showed excellent agreement in segmentation for centerline computation in zones A, B, and C: 0.98 (95% CI 0.97 to 1.00), 0.98 (95% CI 0.97 to 0.99), and 0.97 (95% CI 0.96 to 0.98), respectively. Interobserver analysis similarly demonstrated good agreement, with ICC indexes of 0.98 (95% CI 0.98 to 0.99), 0.95 (95% CI 0.94 to 0.97), and 0.94 (95% CI 0.94 to 0.95), respectively.

Discussion

The current study focused on the evaluation of morphological changes in the femoropopliteal segment due to limb flexion in patients undergoing PAA repair with a Viabahn stent-graft.

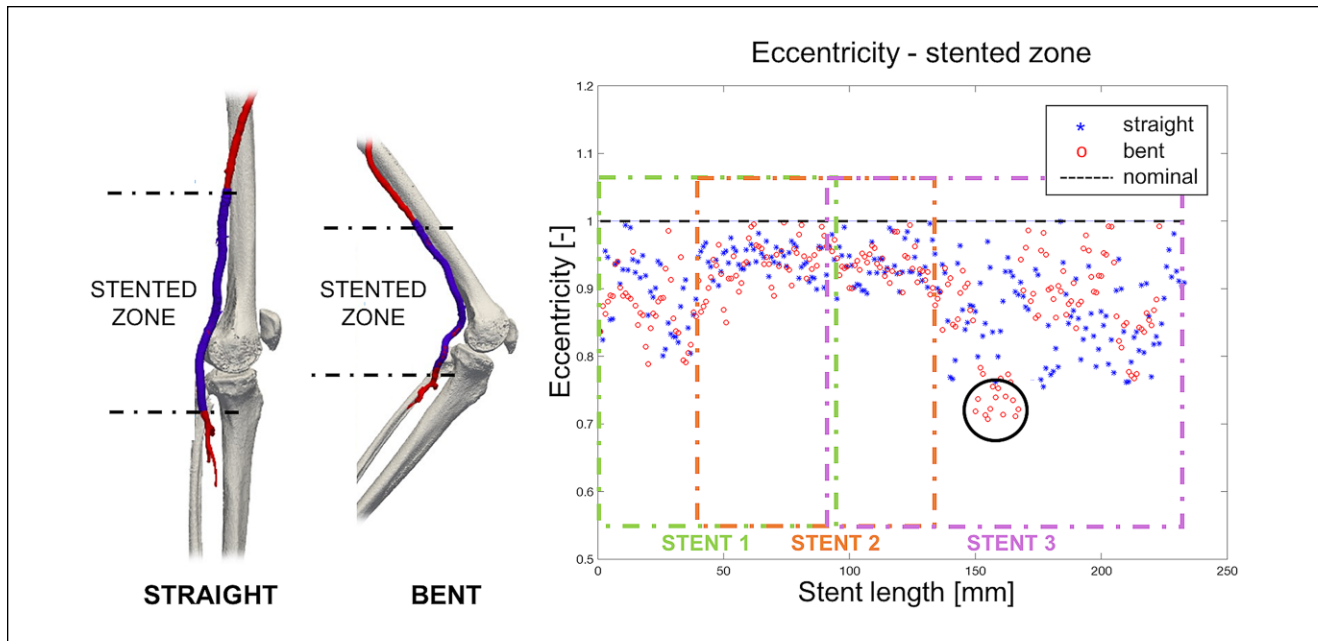


Figure 5. On the left, 3-dimensional reconstruction of bones and the femoropopliteal segment (red) in both straight- and bent-limb configurations from a representative patient. The stent-graft is highlighted in blue. On the right, the graph demonstrates the change in eccentricity along the length of the stent-graft segment in straight and bent positions. The black dashed line denotes eccentricity of an ideal circular section. The black circle highlights the zone where eccentricity reduction was observed during limb flexion. Colored boxes refer to different stents.

Prior *in vivo* studies investigating deformations of the FP segment during limb flexion mainly utilized young healthy volunteers, which did not allow the assessment of age and arterial pathology on vessel kinematics.^{9,10} *Ex vivo* studies in older cadavers¹¹ have been reported as well, but the absence of active muscle contraction may potentially affect limb flexion-induced deformations.¹² On this premise, Gökgöl et al¹³ quantified popliteal artery deformation during in leg flexion in subjects with occlusive PAD. More recently, the same team¹⁵ studied FP deformation in patients before and after stent placement for occlusive disease. However, no one to our knowledge has investigated *in vivo* PAA repair in the context of limb flexion.

This study utilized a novel protocol for CTA acquisition in both bent- and straight-leg positions, which optimized the amount of contrast for imaging the vessel lumen from the aorta to the DPA.²¹ In general, 100 to 130 mL of contrast medium is recommended to obtain a good quality CTA, but several reports suggest lower contrast concentrations.²² Our study employed a double scan, low-dose contrast and radiation protocol to analyze peripheral arteries of the lower limbs in standardized 90° and 180° positions, achieving excellent image quality. The protocol for obtaining a bent-limb CTA also allowed assessment of arterial curvature and tortuosity, which were previously reported as risk factors for arterial pathology in patients undergoing stenting.²³

Our results demonstrate that proximal to the stent-grafts, the arterial diameter, eccentricity, and mean centerline curvature of the FP segment does not change significantly with limb flexion, but the vessel section foreshortens an average of 6%. This value is in line with previously reported findings by Choi et al¹⁰ ($8.8\% \pm 4.4\%$), Ansari et al²⁴ (4%–6%), and Ni Ghriallais et al²⁵ ($9.9\% \pm 1.8\%$), who also analyzed long arterial segments. However, the value is lower than segmental values reported by Poulson et al,²⁶ likely due to nonuniform distribution of FP deformations along the length of the arteries.

In the repaired zone, the stent-graft mean diameter reduced 3% during limb flexion, but mean and minimum eccentricity did not change significantly, suggesting that the Viabahn stent-graft generally remains circular during flexion of the limb. In some patients, however, localized areas of eccentricity reduction were detected in this zone, which shows the tendency of the stent-graft to pinch in the flexed limb posture, as also reported previously.^{12,27}

The stent-grafted zone foreshortened on average 4% during limb flexion, which is in line with previously reported data for the non-stented arteries reported by Ansari et al.²⁴ Using a heterogeneous group of patients with and without PAD, as well as human cadavers, this group reported an axial shortening of 4% to 13.9% in the FP segment depending on the axial position along the vessel. Comparison of our data to these results suggests that

the implanted stent-grafts were able to maintain these baseline values of physiological foreshortening. The capability of the Viabahn to avoid foreshortening has also been confirmed by MacTaggart et al¹² in cadaver models. Similar findings were found with regards to curvature and tortuosity, whose variations between straight and bent configurations reflect the outcomes of unstented zone A. Unfortunately, no direct comparison is possible with other published articles in the case of PAAs.

Though no statistical significance was reached, the largest change in vessel foreshortening was observed distal to the stent-graft in zone C. In this section, the vessel foreshortened on average 8%, which is in line with the results that MacTaggart et al¹² measured in perfused cadavers. Moreover, an average diameter reduction of 1.25% was detected distally to the stent in our series. A possible explanation is that in this area the subarticular popliteal artery is less affected by the presence of muscle mass, so it is more physiologically subject to variations during flexion. It is also important to note that the average length of zone C was only 4.5 ± 3.6 cm, which is 5-fold shorter than the lengths of zones A or B. This smaller length and large variation may have contributed to the lack of statistical significance.

Limitations

While our study describes morphological changes to endovascularly-repaired PAAs during limb flexion, its findings need to be considered in the context of study limitations. First and foremost, only a small number of patients could be recruited for the study. Though PAAs are the most frequently encountered peripheral aneurysms, the overall prevalence is low (<1%). Furthermore, not all patients are treated endovascularly, and of those who are, some are unable to undergo postoperative CTA. All these factors significantly reduced our sample size, and larger studies are required to validate our conclusions.

The second limitation is related to the heterogeneity in patient conditions and repair configurations. As demonstrated in Figure 3, there was a significant difference in the location, length, and number of stent-grafts between all 7 patients, producing an appreciable variation in the lengths of zones A, B, and C. This limitation is particularly important as the FP segment is known to deform nonuniformly along its length.¹¹

Another limitation is related to comparisons of our results with the literature, which is composed of very inhomogeneous data including different disease pathologies, age, and vessel type. To address this, future assessments should also include preoperative bilateral bent-limb scans that can act as a proper baseline for postoperative comparisons. Such studies will also be able to assess the effects of surgical exposure of the proximal SFA on arterial deformations, an aspect that has not been evaluated here.

Finally, future work will include the analysis of arterial hemodynamics in the bent-limb configuration, as previously done for the nonstented artery,²⁸ and utilize arterial landmarks to assess arterial twist during flexion of the limbs.²⁹ While these limitations are being addressed, our work provides the initial assessment of FP biomechanics in patients with endovascularly repaired PAAs and describes a CTA protocol to perform this 3D assessment.

Conclusion

The in vivo behavior of the FP segment was characterized during limb flexion in patients undergoing endovascular treatment of PAAs with a Viabahn stent-graft. The results demonstrate that limb flexion causes arterial foreshortening and increases mean curvature and tortuosity both within and outside of the repaired arterial segment. Presented data can be used in structural and hemodynamic simulations to assess device-artery interactions in the flexed-limb posture and to investigate the ability of stent-grafts to avoid mechanical failure.^{16,30}

Acknowledgments

The authors acknowledge Ana Jornea (University of Pavia) for her support in the analysis procedure.


Declaration of Conflicting Interests

The author(s) declared no potential conflicts of interest with respect to the research, authorship, and/or publication of this article.

Funding

The author(s) disclosed receipt of the following financial support for the research, authorship, and/or publication of this article: Alexey Kamenskiy was supported in part by the National Heart, Lung, and Blood Institute of the National Institutes of Health (NIH) under Award Number R01 HL125736. In accordance with the NIH Public Access Policy, this article is available for open access at PubMed Central.

ORCID iD

Giovanni Spinella  <https://orcid.org/0000-0001-6373-0199>

References

1. Tuveson V, Löfdahl HE, Hultgren R. Patients with abdominal aortic aneurysm have a high prevalence of popliteal artery aneurysms. *Vasc Med*. 2016;21:369–375.
2. Pulli R, Dorigo W, Castelli P, et al. A multicentric experience with open surgical repair and endovascular exclusion of popliteal artery aneurysms. *Eur J Vasc Endovasc Surg*. 2013;45:357–363.
3. Gerasimidis T, Sfyroeras G, Papazoglou K, et al. Endovascular treatment of popliteal artery aneurysms. *Eur J Vasc Endovasc Surg*. 2003;26:506–511.

4. Wrede A, Wiberg F, Acosta S. Increasing the elective endovascular to open repair ratio of popliteal artery aneurysm. *Vasc Endovasc Surg*. 2018;52:115–123.
5. Lovegrove RE, Javid M, Magee TR. Endovascular and open approaches to non-thrombosed popliteal aneurysm repair: a meta-analysis. *Eur J Vasc Endovasc Surg*. 2008;36:96–100.
6. Leake AE, Segal MA, Chaer RA, et al. Meta-analysis of open and endovascular repair of popliteal artery aneurysms. *J Vasc Surg*. 2017;65:246–256.
7. Tielliu IF, Zeebregts CJ, Vourliotakis G, et al. Stent fractures in the Hemobahn/Viabahn stent graft after endovascular popliteal aneurysm repair. *J Vasc Surg*. 2010;51:1413–1418.
8. Tielliu IF, Verhoeven EL, Zeebregts CJ, et al. Endovascular treatment of popliteal artery aneurysms: results of a prospective cohort study. *J Vasc Surg*. 2005;41:561–566.
9. Diehm N, Sin S, Hoppe H, et al. Computational biomechanics to simulate the femoropopliteal intersection during knee flexion: a preliminary study. *J Endovasc Ther*. 2011;3:388–396.
10. Choi G, Cheng CP. Quantification of in vivo kinematics of superficial femoral artery due to hip and knee flexion using magnetic resonance imaging. *J Med Biol Eng*. 2016;36:80–86.
11. MacTaggart JN, Phillips NY, Lomneth CS, et al. Three-dimensional bending, torsion and axial compression of the femoropopliteal artery during limb flexion. *J Biomech*. 2014;47:2249–2256.
12. MacTaggart J, Poulson W, Seas A, et al. Stent design affects femoropopliteal artery deformation [published online March 23, 2018]. *Ann Surg*. doi:10.1097/SLA.0000000000002747
13. Gökgöl C, Diehm N, Kara L, et al. Quantification of popliteal artery deformation during leg flexion in subjects with peripheral artery disease: a pilot study. *J Endovasc Ther*. 2013;20:828–835.
14. Ganguly A, Simons J, Schneider A, et al. In-vivo imaging of femoral artery nitinol stents for deformation analysis. *J Vasc Interv Radiol*. 2011;22:244–249.
15. Gökgöl C, Schumann S, Diehm N, et al. In vivo quantification of the deformations of the femoropopliteal segment: percutaneous transluminal angioplasty vs nitinol stent placement. *J Endovasc Ther*. 2017;24:27–34.
16. Conti M, Marconi M, Campanile G, et al. Patient-specific finite element analysis of popliteal stenting. *Meccanica*. 2017;52:633–644.
17. Antiga L, Piccinelli M, Botti L, et al. An image-based modeling framework for patient-specific computational hemodynamics. *Med Biol Eng Comput*. 2008;46:1097–1112.
18. Besl PJ, McKay ND. Method for registration of 3-D shapes. In: *Sensor Fusion IV: Control Paradigms and Data Structures*. International Society for Optics and Photonics. 1992;1611:586–607.
19. Antiga L, Ene-Iordache B, Remuzzi A. Centerline computation and geometric analysis of branching tubular surfaces with application to blood vessel modeling. Presented at: 11th International Conference in Central Europe on Computer Graphics, Visualization, and Computer Vision; February 3–7, 2003; Plzen-Bory, Czech Republic.
20. Piccinelli M, Veneziani A, Steinman DA, et al. A framework for geometric analysis of vascular structures: application to cerebral aneurysms. *IEEE Trans Biomed Eng*. 2009;28:1141–1155.
21. Fleischmann D, Rubin GD, Bankier AA, et al. Improved uniformity of aortic enhancement with customized contrast medium injection protocols at CT angiography. *Radiology*. 2000;214:363–371.
22. Baxa J, Vendiš T, Moláček J, et al. Low contrast volume run-off CT angiography with optimized scan time based on double-level test bolus technique—feasibility study. *Eur J Radiol*. 2014;83:e147–e155.
23. Tillich M, Bell RE, Paik DS, et al. Iliac arterial injuries after endovascular repair of abdominal aortic aneurysms: correlation with iliac curvature and diameter. *Radiology*. 2001;219:129–136.
24. Ansari F, Pack LK, Brooks SS, et al. Design considerations for studies of the biomechanical environment of the femoropopliteal arteries. *J Vasc Surg*. 2013;58:804–813.
25. Ní Ghriallais R, Heraty K, Smouse B, et al. Deformation of the femoropopliteal segment: effect of stent length, location, flexibility, and curvature. *J Endovasc Ther*. 2016;23:907–918.
26. Poulson W, Kamenskiy A, Seas A, et al. Limb flexion-induced axial compression and bending in human femoropopliteal artery segments. *J Vasc Surg*. 2018;67:607–613.
27. Desyatova A, Poulson W, MacTaggart J, et al. Cross-sectional pinching in human femoropopliteal arteries due to limb flexion, and stent design optimization for maximum cross-sectional opening and minimum intramural stresses. *J R Soc Interface*. 2018;15(145):20180475. doi:10.1098/rsif.2018.0475
28. Desyatova A, MacTaggart J, Romarowski R, et al. Effect of aging on mechanical stresses, deformations, and hemodynamics in human femoropopliteal artery due to limb flexion. *Biomech Model Mechanobiol*. 2018;17:181–189.
29. Desyatova A, Poulson W, Deegan P, et al. Limb flexion-induced twist and associated intramural stresses in the human femoropopliteal artery. *J R Soc Interface*. 2017;14(128):20170025. doi:10.1098/rsif.2017.0025
30. Petrini L, Trotta A, Dordoni E, et al. A computational approach for the prediction of fatigue behaviour in peripheral stents: application to a clinical case. *Ann Biomed Eng*. 2016;44:536–547.